

pubs.acs.org/JPCA Article

Spectroscopy and Photochemistry of OAINO and Implications for New Metal Chemistry in the Atmosphere

Vincent J. Esposito, C. Zachary Palmer, Ryan C. Fortenberry, and Joseph S. Francisco*



Cite This: J. Phys. Chem. A 2023, 127, 7618-7629



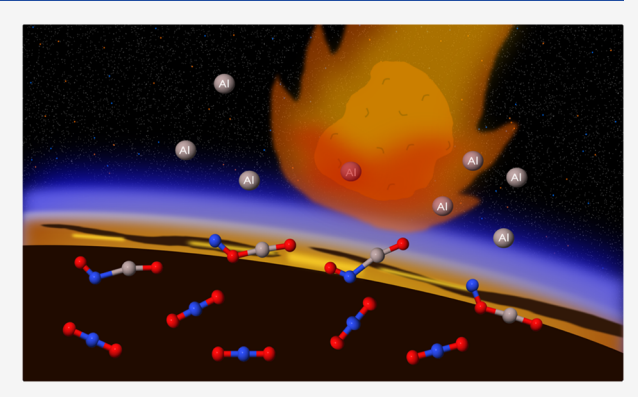
ACCESS I

III Metrics & More

Article Recommendations

s Supporting Information

ABSTRACT: A new aluminum-bearing species, OAlNO, which has the potential to impact the chemistry of the Earth's upper atmosphere, is characterized via high-level, *ab initio*, spectroscopic methods. Meteor-ablated aluminum atoms are quickly oxidized to aluminum oxide (AlO) in the mesosphere and lower thermosphere (MLT), where a steady-state layer of AlO then builds up. Concurrent formation of nitric oxide (NO) in the same region of the atmosphere will lead to the bimolecular formation of the OAlNO molecule. Molecular orbital analysis provides fundamental insights into the chemical bonding and energetic arrangement of the triplet (1 ³A") ground state and singlet (1 ¹A') excited-state species of OAlNO. Additionally, unpaired electrons on the terminal oxygen atom of triplet (1 ³A") OAlNO cause it to be reactive to atmospheric species,



potentially impacting climate science and high-altitude chemistry. The triplet (1 ³A") ground-state species exhibits a large permanent dipole moment useful for rotational spectroscopic detection; however, similar rotational constants to the singlet (1 ¹A') excited-state species will hamper differentiation in a spectrum. Strong infrared intensities will assist in detection and discrimination of the different spin states and isomers. Repulsive electronic excited states of OAlNO will lead to photolysis of the Al–N bond and formation of various electronic states of AlO + NO through nonadiabatic pathways. Reaction through the OAlNO intermediate represents a means for the production of electronically excited AlO, leading to new chemistry in the atmosphere. Excitation to higher-lying electronic states will lead to fluorescence with a minor Stokes shift, useful for laboratory investigation. Such physical properties of this molecule will allow for new, unexplored chemical pathways in the MLT to be considered.

1. INTRODUCTION

Triplet ground states challenged the existing paradigms of electron behavior in the mid 20th century when Mulliken¹ published the first qualitative study of methylene (CH₂), which was later followed by Walsh.² CH₂ is the simplest polyatomic free radical with a triplet ground state garnering notable attention in the years since. Investigations of the CH₂ triplet ground state were overwhelmingly theoretical until 1961, when Herzberg published the first conclusive electronic spectrum of CH₂ in its triplet and singlet states.³ Within the next decade, the nonlinearity of CH₂ resulting from the ¹A₁ ground electronic state was the subject of significant study, both theoretical and experimental. 4-8 This was followed shortly by another experimental study by Herzberg and Johns, confirming the previous theoretical and experimental suggestions that the ground state of CH₂ is not linear, with a ³B₁ term⁹ exposing the importance of the interplay between theory and experiment. 10-12

The story of CH_2 has laid the foundation for the future exploration of other triplet ground-state molecules. One notable example of triplet chemistry from fundamental organic chemistry is tetramethylenemethane (C_4H_6) , 13 a prototypical π -system hydrocarbon stabilized by three resonance structures.

Longitudinal studies have also highlighted that organic silylenes, which are necessary for industrial silicone chemistry, commonly exihibit triplet ground states. ¹⁴ Additionally, platinum nitrene complexes that participate in nitrogen atom transfer reactions due to the subvalency of the Pt–N bonds are also well known for their triplet, electronic ground states. ¹⁵ As a result, the unique properties and reactivity of triplet ground-state molecules produce novel chemistry.

Such behavior extends to aluminum-bearing molecules as well. For instance, recent studies have identified triplet ground states in small, aluminum-bearing molecules such as AlCH, AlOP, and AlNO. These small structures highlight that simple aluminum compounds appear to prefer to create triplet states instead of producing higher bond orders. The question of course, remains as to whether or not such behavior

Received: July 1, 2023 Revised: August 14, 2023 Published: August 30, 2023





is standard in only small, Al-terminated molecules or if this is present in other Al-containing molecules. Only more data on such species can provide insights into this query.

Aluminum is a common material colloquially associated with single-use beverage containers but is a bulk material of significant note in manufacturing. Beyond these anthropocentric uses for element-13, Al is also common in the earth's lithosphere and in the local cosmic neighborhood. Aluminum is present in the earth's atmosphere, delivered via ablation of meteors and cosmic dust at altitudes between 80 and 120 km above sea level, a region typically called the mesosphere/lower thermosphere (MLT).²² For elements such as Mg, Fe, and Na, this produces atmospheric layers of free neutral and ionized atoms, 23 but the case of Al is different. Aluminum undergoes rapid reaction with the abundant O2 molecule, producing a layer of aluminum oxide (AlO) in the MLT.²⁴ This AlO is then available for chemical reactions with other species present in this region. Beyond this major AlO product, MLT chemistry involving Al, C, and O chemical reactions with O2, CO2, and O₃ (among others) supports the idea that AlOH and Al⁺, along with AlO, are the three major Al-containing species present above 80 km, according to theoretical and experimental analysis by Plane and Mangan et al. AlO₂ may exist as well, but its predicted abundance is not as clearly constrained.^{24,25}

This Al + C/O chemistry^{24–26} has been more extensively explored than Al reactions involving nitrogen. Nitrogen, of course, is more abundant in the earth's atmosphere, but reactive nitrogen atoms are present in certain regions at highenough concentrations to make a difference in aluminum chemistry. Nitric oxide (NO) is produced from the reaction of excited N (²D) atoms and molecular oxygen according to the reaction²⁷

$$N(^{2}D) + O_{2} \rightarrow NO + O$$
 (R1)

This excited atomic nitrogen is created by the dissociation of N₂ upon collision with either auroral electrons or electrons stemming from extraterrestrial, soft X-ray ionization of thermospheric, neutral species.²⁸ NO is also destroyed via solar photolysis, implying that a balance exists between production and destruction of NO due to solar activity. Even so, the concentration of NO in the atmosphere is drastically affected by daily and even seasonal changes in solar activity. The mean NO density in the MLT as measured from 2004 to 2016 at altitudes from 85 to 120 km indicates a maximum value of up to 16×10^7 cm⁻³ and occurs at around 70° magnetic latitude at an altitude of approximately 102 km. High densities of $\sim 10-12 \times 10^7$ cm⁻³ also can occur at an altitude of 90 km.²⁷ These measurements place the highdensity regions of NO at similar altitudes in the AlO layer, again produced by meteoric ablation suggesting the possibility of reactions between the two diatomic oxides.

The reaction of AlO + NO is theorized here to proceed through the [Al, N, O_2] reactive intermediate, which may be thermalized in the earth's atmosphere via the following pathway

$$AIO + NO \rightarrow AINO_2^*$$
 (R2)

$$AlNO_2^* + M \rightarrow AlNO_2$$
 (R3)

where M is some inert gas such as N₂ (when not under auroral or X-ray exposure) and AlNO₂* represents internal excitation. The ground state for the AlNO₂ molecule is initially hypothesized here to be a triplet, continuing the trend seen

with other Al-bearing compounds for this naturally occurring molecule. Previous studies of Al compounds 16,17 have not provided chemical explanations for the higher stability of the triplet ground state, nor have they spoken to their possible atmospheric implications. Herein, high-level *ab initio* methods are employed to explore the electronic structure of the novel [Al, N, O_2] molecular system as well as providing the needed reference data for its possible *in situ* observations. Such data will provide further insights into the nature of the Alcontaining, triplet ground state, small molecules and will subsequently provide comment on how such molecules may affect the chemistry of the earth's upper atmosphere.

2. COMPUTATIONAL METHODS

The different singlet and triplet isomers of the [Al, N, O₂] molecular system are searched using B3LYP density functional theory.²⁹ Once the stable isomers are identified, they are optimized using coupled cluster theory, including full treatment of single and double excitations along with perturbative treatment of triples (CCSD(T)), 30,31 in conjunction with the ladder of augmented correlation consistent basis sets, aug-ccpV(X+d)Z (X = T, Q, 5).³² Additional tight d functions are added to the aluminum atom to properly describe its electronic structure.³³ Explicit treatment of the electron correlation is included using the CCSD(T)-F12b formalism^{34,35} with correlation consistent, explicitly correlated basis sets ccpVXZ-F12 (X = D, T, Q). The total energies and geometrical parameters are then extrapolated to the complete basis set limit using the two-point extrapolation scheme: E(x)= E_{CBS} + $BX^{-\alpha}$, where E(x) is the *ab initio* value for a given basis set, X is the cardinal number of the basis set, E_{CBS} is the extrapolated parameter, and B and α are fitting parameters. The equilibrium permanent dipole moment for each isomer is calculated with the CCSD(T)-F12b/cc-pVQZ-F12 level of theory using the finite field procedure (field strengths of 0, 0.005, -0.005 au) as implemented in MOLPRO2021.37 Natural bond orbital (NBO) analysis³⁸ is also performed for 1 3A" and 1 1A' states of OAlNO at the B2PLYP-D3/aug-ccpV(T+d)Z level of theory^{39,40} in Gaussian16.⁴¹

Of the stable isomers investigated in this work, the lowest energy structures, the 1 ¹A' and 1 ³A" states of OAlNO, and the 1 ³A" state of OAlON, from Figure 1 are selected to investigate their rovibrational spectroscopic characteristics for detection in the laboratory, Earth's atmosphere, and potentially in astrophysical environments beyond. To that end, rovibra-

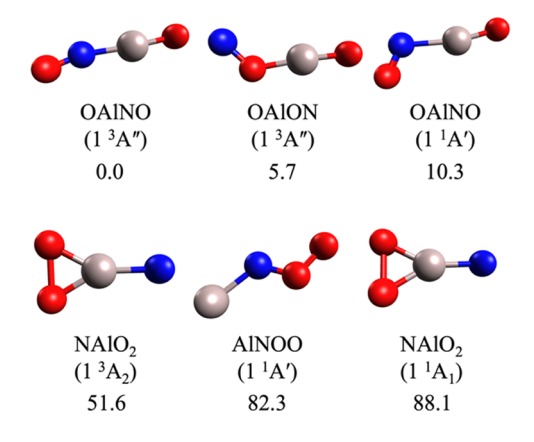


Figure 1. Structures and stability of [Al, N, O_2] isomers with energies in kcal mol⁻¹ at the CCSD(T)-F12b/CBS level.

tional reference data are provided herein *via* quantum chemical calculations known as quartic force fields (QFFs). A QFF is a fourth-order Taylor series expansion to the potential energy portion of the internuclear Watson Hamiltonian. ⁴² QFFs are well known to yield highly accurate anharmonic fundamental vibrational frequencies along with ground and vibrationally excited-state rotational constants within 1% of experimental data for a plethora of chemical systems. ^{43–53} The computed QFFs in this work are produced in conjunction with electronic structure computations that provide the rovibrational reference data necessary for the laboratory or atmospheric detection of the three lowest energy isomers of these unique aluminum-containing species.

The present rovibrational study utilizes a QFF method based on CCSD(T)54 again within the explicitly correlated F12b formalism^{34,35} conjoined to the corresponding cc-pVTZ-F12 basis set. This QFF is typically called "F12-TZ." While the F12-TZ QFF has been used in the past to provide accurate anharmonic fundamental frequencies, 55-60 one of its major downfalls is its inability to calculate high-accuracy rotational constants. 56,57,61 In order to overcome the accuracy shortcomings in the rotational constants, a composite method is employed that combines the accuracy in the anharmonic frequencies from the F12-TZ method and the higher accuracies for the rotational constants achieved by a previous and well documented composite method. 53 This QFF method utilized herein uses the CCSD(T)-F12b level with the inclusion of explicit core-electron correlation in the ccpCVTZ-F12 basis set⁶² and scalar relativistic corrections also present in the previous composite methodology. This new composite method will henceforth be abbreviated "F12-TZcCR."63 The F12-TZ-cCR methodology has been previously used to produce more accurate rovibrational spectroscopic data than that of both F12-TZ and other canonical CCSD(T)based composite methods with the added benefit of a decrease in computational cost compared to the composite method.63-65 Consequently, the F12-TZ-cCR QFF is employed herein to provide accurate predictions for the rovibrational character of the aluminum-containing species investigated in this work.

The F12-TZ-cCR QFF computations begin with the optimization of the molecular geometry of the first three lowest energy isomers of the [Al, N, O₂] molecular system with exceptionally tight convergence criteria at the CCSD(T)-F12b/cc-pCVTZ-F12 level of theory utilizing the MOLPRO 2020.1 quantum chemical package.⁶⁶ The optimized geometries are then displaced by 0.005 Å or radians, depending on bond lengths or angles/torsions, using their symmetry-internal coordinates via the INTDER program.⁶⁷ The three lowest energy isomers of the aforementioned molecular system are of the same connectivity as a previously studied Al-containing species, ⁶⁸ which allows for a similar coordinate scheme to be used that make up 743 symmetry-unique points and should be understood to be the standard bond lengths and angles. For the 1 ³A" and 1 ¹A' states corresponding to OAlNO (defined in the next section), the following simple-internal coordinate (SIC) system is used

$$S_{1} = r(O_{1}-AI)$$

$$S_{2} = r(AI-N)$$

$$S_{3} = r(N-O_{2})$$

$$S_{4} = \angle(AI-N-O_{2})$$

$$S_{5} = LINX(O_{2}-N-AI-O_{1})$$

$$S_{6} = LINY(O_{2}-N-AI-O_{1})$$

For OAlON, the following simple-internal coordinate system is used

$$S_{1} = r(O_{1}-AI)$$

$$S_{2} = r(AI-O_{2})$$

$$S_{3} = r(O_{2}-N)$$

$$S_{4} = \angle(AI-O_{2}-N)$$

$$S_{5} = LINX(N-O_{2}-AI-O_{1})$$

$$S_{6} = LINY(N-O_{2}-AI-O_{1})$$

The LINX and LINY coordinates are displacements from linearity in and above the plane of the molecule, respectively, as discussed in ref 67.

Single-point energy (SPE) calculations are then computed at every displacement with the same level of theory as the geometry optimizations, also using the MOLPRO suite. 66 The F12-TZ-cCR SPE calculations also include the Douglas-Kroll scalar relativistic corrections⁶⁹ computed from the difference in energies at the CCSD(T)/cc-pVTZ-DK level of theory with the use of the second-order Douglas-Kroll-Hess Hamiltonian turned on or off. Once the SPEs of the F12-TZ-cCR QFF are computed, the energies are then fit using a least-squares procedure with sums of squared residuals on the order of 10^{-16} au² and lower in some cases. This fit computes a corrected Hessian matrix that is used in a second fitting to produce the final equilibrium geometry and force constants from the produced zero gradients. These gradients are then transformed from SICs into Cartesian coordinates through the INTDER program.⁶⁷ The new Cartesian force constants are employed by the SPECTRO program⁷⁰ to produce anharmonic fundamental vibrational frequencies, two-quanta overtones and combination bands, and rotational constants generated by rotational and vibrational perturbation theory at secondorder (VPT2).71-73

Additionally, the rovibrational spectra for the Al-containing species studied herein are further corrected by the SPECTRO program's ⁷⁰ ability to treat Fermi resonances and resonance polyads. Furthermore, dipole moments for each isomer are computed at the CCSD(T)-F12/cc-pCVTZ-F12 level of theory using the MOLPRO suite. ⁶⁶ Also, anharmonic infrared intensity calculations are carried out at the B3LYP/aug-cc-pVDZ level of theory ²⁹ utilizing the Gaussian16 suite of quantum chemical packages. ⁴¹ Intensity calculations at lower levels of theory have been shown to produce semi-quantitative agreement with higher levels of theory for far less computational cost. ^{74–77} Infrared transition intensities are proportional to the change in the dipole moment for a given vibrational transition, therefore being more significant for molecules with larger dipole moments.

Table 1. Geometry Parameters for the Isomers of [Al, N, O_2]^{a,b}

| Isomer | Method | $R_{ m NO1}$ | $R_{ m AlN}$ | R_{AlO2} | $\angle O_1$ -N-Al | $\angle N-Al-O_2$ | τ | $E_{ m rel}$ |
|---------------------------|---------------------------------|------------------|------------------|---------------------|--------------------|-------------------------|----------------|--------------|
| OAlNO $(1 {}^{3}A'')$ | CCSD(T)/CBS | 1.2031 | 1.7565 | 1.6029 | 166.1 | 176.4 | 180.0 | 0.00 |
| | CCSD(T)-F12b/CBS | 1.2030 | 1.7568 | 1.6020 | 165.7 | 176.5 | 180.0 | 0.00 |
| OAlNO $(1 {}^{1}A')$ | CCSD(T)/CBS | 1.2080 | 2.0057 | 1.6055 | 116.8 | 170.4 | 180.0 | 10.3 |
| | CCSD(T)-F12b/CBS | 1.2078 | 2.0050 | 1.6058 | 116.7 | 170.5 | 180.0 | 10.6 |
| Isomer | Method | R_{NO1} | R_{AlO1} | R_{AlO2} | $\angle N-O_1-Al$ | $\angle O_1$ -Al- O_2 | τ | $E_{ m rel}$ |
| OAION $(1 {}^{3}A'')$ | CCSD(T)/CBS | 1.3178 | 1.7158 | 1.6012 | 127.4 | 176.2 | 180.0 | 6.0 |
| | CCSD(T)-F12b/CBS | 1.3169 | 1.7148 | 1.6013 | 127.4 | 176.2 | 180.0 | 5.9 |
| Isomer | Method | $R_{\rm NO1}$ | $R_{ m AIN}$ | $R_{\rm O1O2}$ | $\angle Al-N-O_1$ | $\angle N-O_1-O_2$ | τ | $E_{ m rel}$ |
| AlNOO (1 ¹ A') | CCSD(T)/CBS | 1.2713 | 1.8955 | 1.3129 | 125.6 | 117.6 | 180.0 | 82.1 |
| | CCSD(T)-F12b/CBS | 1.2706 | 1.8956 | 1.3133 | 125.6 | 117.6 | 180.0 | 82.3 |
| Isomer | Method | R_{AlO1} | $R_{ m AlN}$ | R_{OO} | $\angle N-Al-O_1$ | ∠Al-O-O | τ | $E_{ m rel}$ |
| $NAlO_{2} (1^{3}A_{2})$ | CCSD(T)/CBS | 1.6958 | 1.8712 | 1.6583 | 150.7 | 60.9 | 180.0 | 51.6 |
| 2 \ 2/ | | | | | | | | |
| 2 (2/ | CCSD(T)-F12b/CBS | 1.6960 | 1.8716 | 1.6574 | 150.7 | 60.9 | 180.0 | 51.6 |
| $NAlO_2 (1 ^1A_1)$ | CCSD(T)-F12b/CBS CCSD(T)/CBS | 1.6960 1.6979 | 1.8716 1.8479 | 1.6574 1.6495 | 150.7 150.9 | 60.9 60.7 | 180.0 180.0 | 51.6 88.1 |

[&]quot;Bond lengths in angstrom and angles in deg, energy in kcal mol⁻¹ and includes harmonic ZPVE. ${}^bR_{xy}$ is bond length; \angle represents the angle between three atoms; τ is the dihedral angle.

Finally, the vertical excitation energies (VEE) and oscillator strengths for spin-allowed transitions to low-lying singlet and triplet states are calculated for ground-state OAlNO using energies from the internally contracted multireference configuration interaction method, 78-80 including the Davidson correction to the energy (MRCI+Q)⁸¹ in conjunction with the aug-cc-pV(T+d)Z basis set and complete active space selfconsistent field (CASSCF) transition dipole moments. These calculations are based on a 12 state-averaged (6 a' and 6 a") CASSCF^{82,83} wavefunction utilizing an active space of 14 electrons in 11 orbitals. This includes occupying 17 a' and 5 a" orbitals while closing the lowest 10 a' and 1 a" orbitals. Following this, one-dimensional (1D) adiabatic potential energy surfaces are calculated for the triplet and singlet states of OAlNO along the O-Al, Al-N, and N-O bond coordinates by performing MRCI+Q/aug-cc-pV(T+d)Z single-point energy calculations at progressively longer bond distances while keeping all other coordinates fixed at their equilibrium value.

3. RESULTS AND DISCUSSION

3.1. Stability and Bonding. Four stable isomers of the [Al, N, O_2] molecular system are found as well as two stable excited states. Their structures are shown in Figure 1. The equilibrium geometries and harmonic zero-point-corrected relative energies of these molecules calculated at the CCSD(T) and CCSD(T)-F12b levels of theory are reported in Table 1.

OAlNO (1 3 A") is the ground state of the system and is quasilinear with \angle O-N-Al and \angle O-Al-N bond angles of 165.7 and 176.5° at the CCSD(T)-F12b/CBS level of theory. The 1 3 A" ground electronic state indicates that if the molecule were linear, the two electrons would both be spin-up in the degenerate π orbitals. The competition between the preference of aluminum to bend along with the linear π orbital construction results in this near-linear nature of the angles. OAlNO (1 3 A") is most likely formed by the AlO + NO reaction discussed previously and has an Al-N bond dissociation energy (BDE) of 27.3 kcal mol⁻¹. Both the Al-O and N-O bonds are much stronger, with BDEs of 121.2 and 163.8 kcal mol⁻¹, respectively. All of these bonds are orders of magnitude stronger than the amount of available energy in the

MLT (approximately 0.5 kcal mol^{-1}). The 1 $^{1}\text{A}'$ state of OAlNO lies 10.6 kcal mol^{-1} above OAlNO (1 $^{3}\text{A}''$) and represents an electronic excited state. In the 1 $^{1}\text{A}'$ state, the $\angle\text{O-N-Al}$ angle shifts to 116.7°, classifying the molecule in this state as an asymmetric top. The AlN bond is also 0.2482 Å longer in the 1 $^{1}\text{A}'$ state at the CCSD(T)-F12b/CBS level of theory.

A natural bond orbital (NBO) analysis for the 1 ³A" and 1 ¹A' states of OAlNO aids in explaining why the 1 ³A" state is more stable than the 1 1A' state. The orbitals are depicted in Figure 2 in energy order, with each orbital's occupancy shown. Drastically different bonding characteristics are present between each spin state. First, both states have an almost isoenergetic $\sigma_{\rm NO}$ bonding orbital, although the orbital in the triplet state is slightly more stable. The almost 0.25 Å difference in the R_{AlN} bond length is borne from the much more stable σ_{AlN} bonding orbital in the 1 $^3A''$ state compared to the 1 ¹A' state. One of the major differences between the two spin states is the bond order of the NO and AlO bonds. The 1 ³A" state has an NO triple bond seen in the doubly occupied σ_{NO} orbital that represents a mildly polar sigma bond with 55% of the bond density localized on the more electronegative oxygen atom and the two doubly occupied π_{NO} orbitals in Figure 2. An AlO single bond stems from the lone σ_{AlO} bonding orbital. Alternatively, the 1 $^1A'$ state has an AlO triple bond and NO double bond. The NO σ and π bonds are quite polar, with a N/O bond weighting percentage of 43/57 and 41/59, respectively. Interestingly, the three doubly occupied AlO bonding orbitals, a σ orbital and two π orbitals, have extremely polar covalent bonds, with the σ_{AlO} having 85% of the bonding interaction localized on the oxygen and the two π_{AlO} bonding orbitals exhibiting 93% oxygen localization. This difference in bond character leaves the 1 ¹A' state with two higher energy π_{AlO} bonding orbitals. Finally, the 1 ${}^3A''$ state has two unpaired electrons in orthogonal oxygen p-orbitals that will cause the 1 3A" state to be more reactive with free radicals than the singlet state.

Moving to the next isomer in Figure 1, OAlON (1 ³A") is 5.9 kcal mol⁻¹ higher in energy than ground-state OAlNO (1 ³A") and can similarly be formed through the AlO + NO reaction but from the inverted angle of attack. The difference

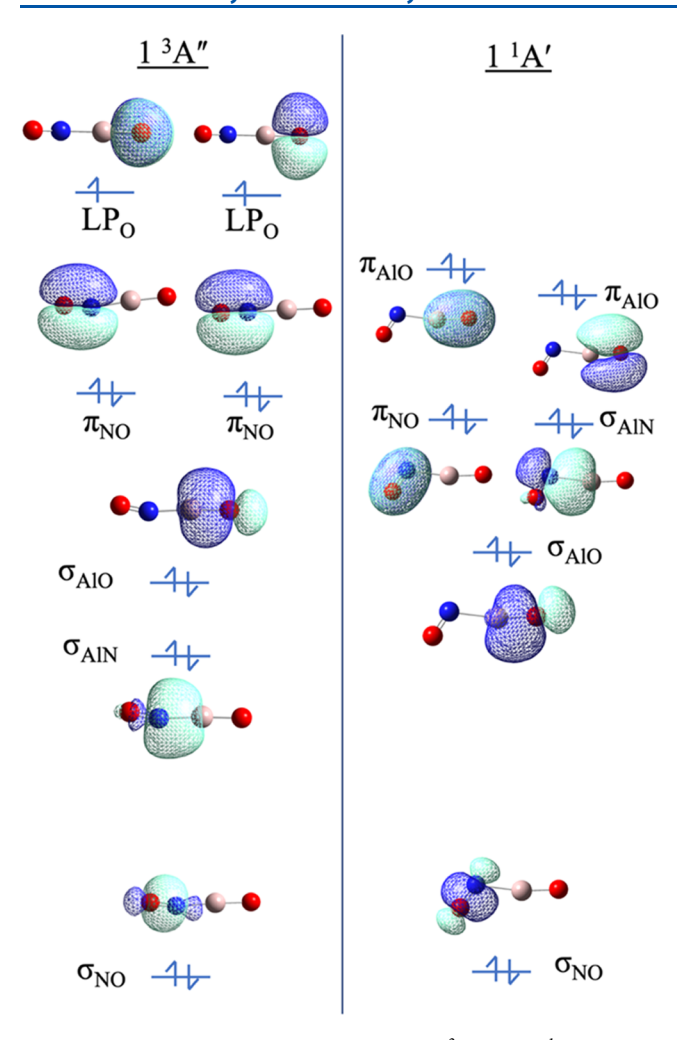


Figure 2. Frontier molecular orbitals of the 1 $^3A''$ and 1 $^1A'$ states of OAlNO from NBO analysis.

in bonding causes major changes in the electronic structure. The terminal $R_{\rm NO}$ bond is predicted to be 1.2030 Å in ground-state OAlNO (1 3 A"), while the change from an internal AlN bond to an internal AlO bond causes the terminal $R_{\rm NO}$ bond to elongate to 1.3169 Å in OAlON (1 3 A") at the CCSD(T)-F12b/CBS level. The NO flip also causes OAlON (1 3 A") to bend away from linearity to a much greater extent than the other isomer with an \angle AlON bond angle of 127.4°.

The next-most stable isomer is NAlO₂ (1 3 A₂), which may be formed through different reaction channels from the previous two isomers, such as N + AlO₂, in the atmosphere and interstellar medium. NAlO₂ (1 3 A₂) is predicted to be 51.6 kcal mol⁻¹ above the ground state, a relatively large gap when compared with the two lower energy isomers. The electronically excited state, NAlO₂ (1 1 A₁), was also identified and lies 36.5 kcal mol⁻¹ above the 1 3 A₂ isomer at 88.1 kcal mol⁻¹ above the lowest energy isomer.

The final isomer determined to be a minimum, AlNOO, is the only one that is found to possess a $^1A'$ ground state. AlNOO (1 $^1A'$) is predicted to have a relative energy of 82.3 kcal mol $^{-1}$ compared to OAlNO (1 $^3A''$). Formation channels for this molecule are unclear, although the reaction of Al + NO₂ or AlN + O₂ could be possible entrance channels. These reactions are unlikely to take place in the earth's atmosphere due to the depletion of Al atoms via rapid oxidation to AlO 24 and the dearth of data on the existence of the AlN diatomic in

the atmosphere. Searches for other isomers such as both spin states of $NAIO_2$ and singlet OAION have been, as of yet, unsuccessful or have been found to be higher-order stationary points characterized by imaginary frequencies. The present ordering is reminiscent of that in ref 68, where the X-AlO $_2$ cyclic forms are less favored than the more linear atomic arrangements.

3.2. Ground-State Spectroscopy. The anharmonic vibrational frequencies and higher-order rotational spectroscopic data for the three lowest energy species (OAlNO $(1^{3}A'')$, OAlON $(1^{3}A'')$, and OAlNO $(1^{1}A')$) are given in Tables 2 and 3. These molecules are chosen for further spectroscopic characterization since they are the products of the proposed AlO + NO reaction, are the lowest energy isomers, and such characterization will allow for the differentiation between the 1 ³A" and 1 ¹A' states of OAlNO. Additionally, the anharmonic ZPVE-corrected, F12-TZ-cCR relative energy of each molecule is given in Table 3 and agrees well with the energetics from Figure 1. The 1 ³A" state of OAlNO is still suggested to be the lowest energy structure, followed by the 1 3A" state of OAlON at 6.0 kcal mol-1 and the 1 ¹A' state of OAlNO at 10.6 kcal mol⁻¹. Both of the latter two state's relative energies differ from the above CCSD(T)-F12b/CBS energy by only 0.3 kcal mol⁻¹. This is not unexpected, as the QFF energies include corrections from the least-squares fitting algorithm and the anharmonic zeropoint energy. With the addition of these terms, the QFF energies should be considered to be a more accurate prediction of the total energetics of the species investigated, but the previously computed values should be considered as an accurate representation for the other isomers.

As no previous theoretical or laboratory rovibrational characterizations of any [Al, N, O2] isomeric molecular system have been carried out, the computed spectroscopic constants and vibrational frequencies provided in this study provide novel reference benchmark data for potential atmospheric observation and gas-phase analysis. While no previous rotational data for the present molecules have been produced as of yet, previous theoretical^{68,84} and experimental^{85,86} studies have been conducted on pseudo-linear, nearly prolate, Alcontaining species with high accuracy, suggesting that the coupled cluster theory methodology should be just as accurate and reliable for the rotational data of the three isomers in the present study. To that end, spectroscopic constants and geometrical parameters for the three isomers/electronic state are given in Table 2. An immediately noticeable result is the absence of the A rotational constants for the 1 ³A" state of OAlNO. While the 1 ¹A' state of OAlNO and the 1 ³A" of OAION are both considered near-prolate, the equilibrium geometry for the ground 1 ³A" state of OAlNO is almost entirely prolate with its two angles, $\angle(Al-N-O_2)$ and $\angle(O_1-$ Al-N) being 165.22 and 176.09°, respectively. Thus, with such a linear bend, the A rotational constants for this isomer are effectively infinity. Additionally, over half of the vibrationally averaged rotational constants between the 1 ¹A' and 1 ³A" states of OAINO exhibit a similar level of near-prolate behavior that does not seem to be present for OAlON, as discussed above. For example, the B2 vibrationally excited rotational constant only differs by ~4.0 MHz for the two electronic states of OAlNO but differs by more than 400 MHz for the same rotational constant of OAION. Even with the small differences between the rotational constants of the 1 ³A" and 1 ¹A' states of OAlNO, the current high resolution and sensitivity of

Table 2. Geometrical Parameters and Spectroscopic Constants for the Three Lowest Energy Molecular Complexes from F12-TZ-cCR QFF VPT2 Analysis

| | Units | OAlNO $(1 {}^{3}A'')^{a}$ | OAlNO $(1^{-1}A')$ | OAION $(1 {}^3A'')$ | | Units | OAlNO $(1 {}^{3}A'')^{a}$ | OAlNO $(1^{-1}A')$ | OAION (1 3 A") |
|---|-------|---------------------------|--------------------|----------------------------------|------------------------------------|--------------|---------------------------|--------------------|-------------------|
| $R_{\rm e}({\rm O_1-Al})$ | Å | 1.59657 | 1.60013 | 1.59458 | A_4 | MHz | | 87 143.2 | 83 203.2 |
| $R_{\rm e}({\rm Al-N})$ | Å | 1.74944 | 2.00865 | $(Al-O_2)$ | B_4 | MHz | 2683.4 | 2673.7 | 3139.6 |
| D (27 G) | 2 | | | 1.70692 | C_4 | MHz | 2643.4 | 2587.4 | 3006.0 |
| $R_{\rm e}(N-O_2)$ | Å | 1.20226 | 1.20035 | 1.31602 | A_5 | MHz | | 91 185.8 | 88 804.1 |
| $\angle_{e}(Al-N-O_2)$ | deg | 165.22 | 119.07 | (Al-O ₂ -N) 128.02 | B_5 | MHz | 2693.7 | 2680.5 | 3106.3 |
| $\angle_{e}(O_1-Al-N)$ | deg | 176.09 | 165.92 | (O_1-Al-O_2) | C_5 | MHz | 2645.6 | 2604.5 | 2992.2 |
| 2 _e (0] 11 11) | acg | 170.07 | 103.72 | 176.13 | A_6 | MHz | | 90 240.8 | 93 404.8 |
| $A_{\rm e}$ | MHz | | 89 666.1 | 85 936.4 | B_6 | MHz | 2730.4 | 2725.2 | 3161.4 |
| $B_{\rm e}$ | MHz | 2635.2 | 2689.7 | 3080.1 | C_6 | MHz | 2675.3 | 2627.0 | 3017.9 |
| $C_{\rm e}$ | MHz | 2630.4 | 2611.5 | 2973.6 | $\Delta_{ m J}$ | kHz | 0.584 | 2.202 | 3.971 |
| $R_0(O_1-Al)$ | Å | 1.59537 | 1.59351 | 1.59398 | $\Delta_{ m K}$ | MHz | | 118.483 | 269.926 |
| R(Al-N) | Å | 1.7574 | 2.0209 | $(Al-O_2)$ | $\Delta_{ m JK}$ | MHz | -72.175 | -0.613 | -1.678 |
| | | | | 1.71083 | $\delta_{ m J}$ | Hz | 65.4368 | 228.298 | 721.722 |
| $R_0(N-O_2)$ | Å | 1.19215 | 1.19846 | 1.31457 | $\delta_{ m K}$ | kHz | 334.151 | 84.656 | 144.12 |
| $\angle_0(Al-N-O_2)$ | deg | 156.45 | 118.69 | $(Al-O_2-N)$ | $\boldsymbol{\Phi}_{\!\mathrm{J}}$ | mHz | 17.971 | 32.821 | 84.225 |
| $\angle_0(O_1-Al-N)$ | 1 | 174.02 | 1// 44 | 126.19 | $\Phi_{ m K}$ | kHz | | -461.282 | |
| $\angle_0(\mathrm{O}_1 - \mathrm{Al} - \mathrm{N})$ | deg | 174.02 | 166.44 | (O_1-Al-O_2) 176.15 | $\Phi_{\rm JK}$ | Hz | -801.482 | -16.185 | 5.797 |
| A_0 | MHz | | 90 352.9 | 86 232.4 | $\Phi_{	ext{KJ}}$ | kHz | | 3.508 | -13.107 |
| B_0 | MHz | 2683.3 | 2689.2 | 3112.0 | $oldsymbol{arphi}_{	ext{j}}$ | mHz | 4.192 | 8.73 | 22.724 |
| C_0 | MHz | 2638.7 | 2605.6 | 2989.3 | $oldsymbol{arphi}_{ m jk}$ | Hz | | 5.148 | 8.322 |
| A_1 | MHz | | 82 891.3 | 69 237.9 | $oldsymbol{arphi}_{ m k}$ | kHz | 23.736 | 6.244 | 9.473 |
| B_1 | MHz | 2701.9 | 2721.0 | 3172.1 | K | | | -0.99809 | -0.99705 |
| C_1 | MHz | 2647.3 | 2629.2 | 3025.1 | μ_x | D | 0.00 | 0.00 | 0.00 |
| A_2 | MHz | | 91 445.5 | 88 105.3 | μ_y | D | 0.02 | 0.21 | 0.80 |
| B_2 | MHz | 2677.3 | 2673.0 | 3092.5 | μ_z | D | 3.35 | 3.67 | 2.61 |
| C_2 | MHz | 2631.9 | 2591.2 | 2973.3 | $\mu_{ m tot}$ | D | 3.32 | 3.82 | 2.66 |
| A_3 | MHz | | 100 584.7 | 95 231.1 | ^a Cubic and | quartic terr | ns removed | from VPT2 | calculations for |
| B_3 | MHz | 2680.1 | 2660.8 | 3063.2 | coordinates 4 | and 5. | | | |
| C_3 | MHz | 2634.4 | 2583.0 | 2953.7 | | | | | |

Table 3. Vibrational Frequencies and Two-Quanta Modes (cm $^{-1}$), IR Transition Intensities in Parentheses (km mol $^{-1}$), and Relative Energies (kcal mol $^{-1}$) of the Three Lowest Energy Molecules

| mode | OAINO $(1 {}^{3}A'')^{a}$ | OAlNO (1 ¹ A') | OAlON $(1 {}^{3}A'')$ |
|-----------------|---------------------------|---------------------------|------------------------|
| ω_1 (a') | 1777.6 | 1506.9 | 1248.7 |
| ω_2 (a') | 1118.6 | 1078.8 | 1126.3 |
| ω_3 (a') | 568.7 | 410.9 | 636.5 |
| ω_4 (a') | 169.3 | 259.1 | 196.7 |
| ω_5 (a") | 166.4 | 91.1 | 182.3 |
| ω_6 (a') | 53.7 | 57.6 | 76.3 |
| ν_1 (a') | 1717.1 (71) | 1492.1 (682) | 1212 (156) |
| ν_2 (a') | 1104.0 (70) | 1066.1 (18) | 1112.9 (62) |
| ν_3 (a') | 573.7 (17) | 397.2 (24) | 634.8 (19) |
| ν_4 (a') | 208.8 (62) | 241.5 (25) | 196 (57) |
| ν_5 (a") | 217.5 (51) | 77.6 (51) | 189.7 (78) |
| ν_6 (a') | 52.4 (1) | 40.2 (43) | 68.1 (23) |
| $2\nu_1$ | | 2952.2 (29) | |
| $\nu_1 + \nu_4$ | | 1742.1 (16) | |
| $\nu_1 + \nu_5$ | | 1573.3 (19) | |
| $2 u_1$ | 3378.8 (13) | | |
| $2\nu_3$ | | | 1260.2 (132) |
| ZPT | 1940.0 | 1690.0 | 1734.2 |
| rel. energy | 0.00 | 10.6 | 6.0 |
| | | | |

[&]quot;Cubic and quartic terms removed from VPT2 calculations for coordinates 4 and 5.

rotational spectroscopic experiments should be sufficient for characterization in the laboratory and detection in the earth's atmosphere.

In order to assist in the detection of the [Al, N, O₂] complexes in the earth's atmosphere and further laboratory analysis, the vibrational spectra of the three lowest energy states/isomers are provided in Table 3. One drawback of the methodology implemented in the present vibrational study is the inability to effectively model the very floppy bends of the 1 3A" state of OAlNO, much like previously studied Alcontaining species,⁶⁸ and even HOOH.^{58,87} For that reason, for the computed vibrational spectra, the untrustworthy cubic and quartic terms of coordinates 4 and 5 were removed for the 1 ${}^{3}A''$ state of OAlNO and the $\angle(Al-N-O_2)$ and in-plane linear bend, respectively, from the VPT2 calculations. Even then, the vibrational spectrum contains some positive anharmonicities for $\nu_4 - \nu_6$ for OAlNO, but this is expected for near-prolate molecules. ^{47,88,89} A similar issue is present for the 1 ³A" state of OAlON with a positive anharmonicity exhibited for v_5 , the out-of-plane bend, which is, again, expected for these near-prolate species. The other frequencies give no indication of concerning behavior, suggesting that the fundamental, anharmonic, vibrational frequency data should be considered accurate enough for its use as reference benchmark data for atmospheric detection and laboratory analysis. Interestingly, the 1 1A' state of OAlNO is the most wellbehaved of the three isomers investigated, exhibiting no positive anharmonicities. Hence, its vibrational spectrum is

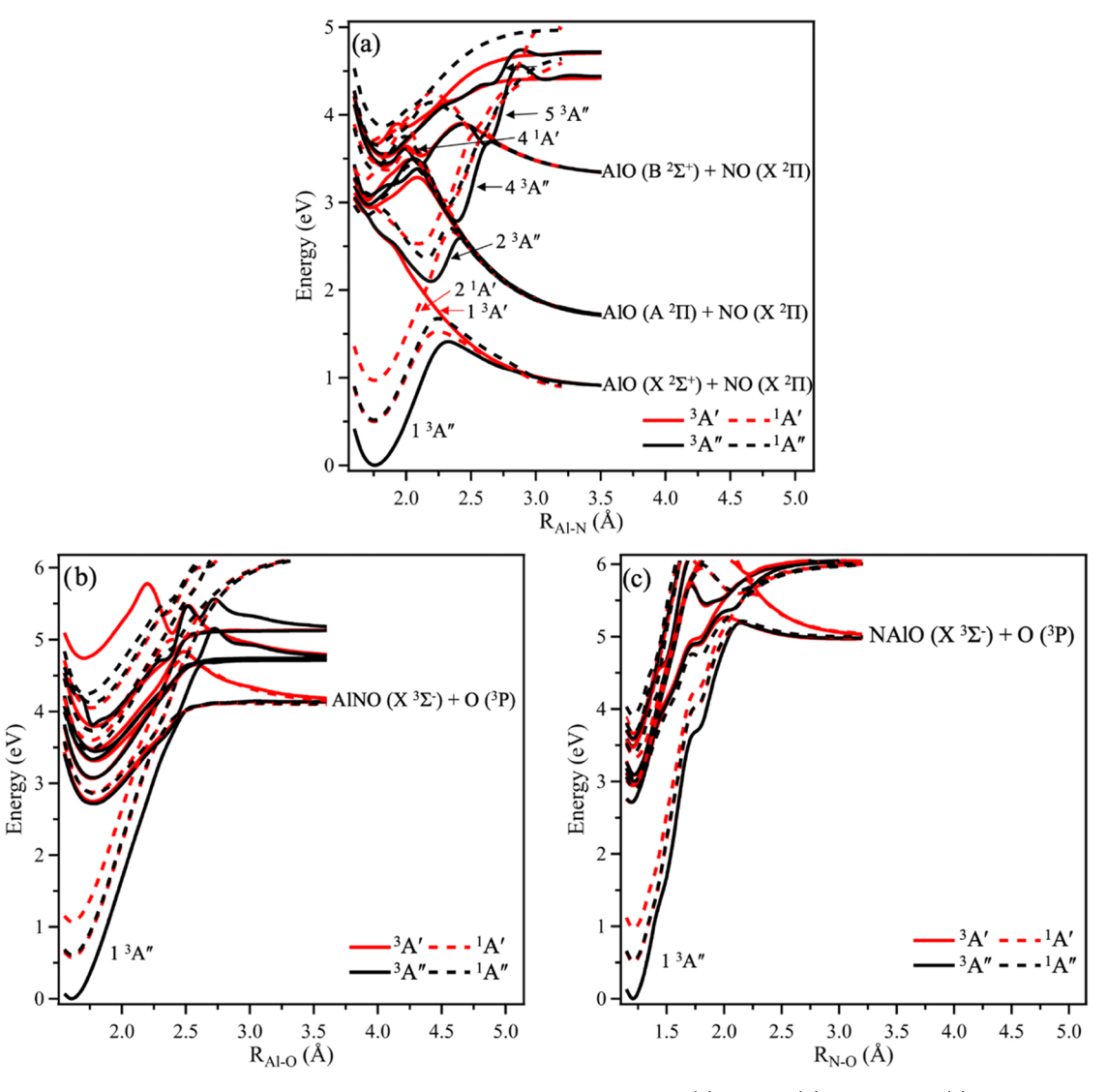


Figure 3. One-dimensional adiabatic potential energy contours of OAlNO along the (a) Al-N, (b) Al-O, and (c) N-O bond coordinates calculated at the MRCI+Q/aug-cc-pV(T+d)Z level of theory. All other coordinates are held fixed at their equilibrium value.

likely the least noisy and most reliable for detection in the infrared.

Moving toward detectability, the 1 ³A" state of OAlNO contains two vibrational frequencies that exhibit transition intensities of ~70 km mol⁻¹, the ν_1 N-O₂ stretch at 1717.1 cm⁻¹ and the ν_2 O₁-Al stretch at 1104.0 cm⁻¹. Both are roughly the same intensity as the O-H anti-symmetric stretch of water, also at roughly 70 km mol⁻¹. For the 1 ³A" state of OAlON, a much brighter 156 km mol⁻¹ transition intensity is exhibited by its ν_1 O₂-N stretch at 1212 cm⁻¹, and additionally, its ν_5 out-of-plane bend at 189.7 cm⁻¹ has a 78 km mol⁻¹ intensity. Furthermore, the 1 ³A" state of OAlON contains a $2\nu_3$ overtone at 1260.2 cm⁻¹ with a transition intensity of 132 km mol⁻¹, a notably detectable feature in this spectral region. The 1 ¹A' state of OAlNO contains the largest vibrational transition intensity in this study at 682 km mol⁻¹ for its ν_1 N-O₂ at 1492.1 cm⁻¹, implying that the region around 6.67 μ m should be a prime candidate for MLT observation for any of these species.

In addition to their intensities, the permanent dipole moments for each molecule are given in Table 2. All three complexes exhibit dipole moments over 2.00 D, with the

largest being the 1 ¹A' state of OAlNO at 3.82 D. These are all considerably larger than the previously studied⁶⁸ AlOH dipole moment of 1.11 D. The higher dipolar features in the present systems are due to the larger charge separation brought about by the presence of a fourth atom as well as the N atom in the present complexes. With each species containing such large dipole moments, atmospheric microwave spectroscopic studies are warranted. That being said, the 1 ¹A' state of OAlNO and the 1 ³A" state of OAlON both contain large vibrational intensities, and their infrared spectral features reported herein should be considered accurate enough to provide reference benchmark data for laboratory comparison and even potential atmospheric or interstellar detection.

3.3. Excited Electronic State Photochemistry of OAINO. Evolution of the low-lying triplet and singlet electronic excited states along the Al–N, Al–O, and N–O bond lengths of OAINO are shown in Figure 3, and the vertical excitation energies and oscillator strengths for the spin-allowed transitions are given in Table 4. Beginning with Figure 3a, the ground 1 $^3A''$ and first excited 1 $^1A''$ states of OAINO adiabatically correlate with the first dissociation limit to form the AlO (X $^2\Sigma^+$) + NO (X $^2\Pi$) products. Both pathways

Table 4. Vertical Excitation Energy (VEE) and Oscillator Strength (f) for Spin-Allowed Triplet and Singlet Transitions of OAlNO Calculated at the MRCI+Q/aug-cc-pV(T+d)Z Level of Theory

| OAINO | | | | | | |
|-------------------|----------|----------|-------|--|--|--|
| | VEE (eV) | VEE (nm) | f | | | |
| 1 ³ A" | 0.000 | | | | | |
| $2^{3}A''$ | 2.714 | 457 | 0.003 | | | |
| 1 ³ A' | 2.718 | 456 | 0.003 | | | |
| $2^{3}A'$ | 2.952 | 420 | 0.003 | | | |
| $3^{3}A'$ | 3.010 | 412 | 0.002 | | | |
| $3^{3}A''$ | 3.100 | 400 | 0.000 | | | |
| $4^{3}A''$ | 3.104 | 399 | 0.038 | | | |
| 5 ³ A" | 3.472 | 357 | 0.011 | | | |
| $4^{3}A'$ | 3.486 | 356 | 0.007 | | | |
| 6 ³ A" | 3.574 | 347 | 0.002 | | | |
| 5 ³ A′ | 3.596 | 345 | 0.000 | | | |
| 6 ³ A′ | 3.664 | 338 | 0.024 | | | |
| | | | | | | |
| 1 ¹ A′ | 0.501 | 2472 | | | | |
| 1 ¹ A" | 0.518 | 2393 | 0.000 | | | |
| 2 ¹ A' | 0.970 | 1278 | 0.000 | | | |
| 2 ¹ A" | 2.903 | 427 | 0.001 | | | |
| 3 ¹ A′ | 2.944 | 421 | 0.002 | | | |
| 3 ¹ A" | 3.060 | 405 | 0.000 | | | |
| 4 ¹ A' | 3.347 | 370 | 0.031 | | | |
| 4 ¹ A" | 3.385 | 366 | 0.001 | | | |
| 5 ¹ A' | 3.453 | 359 | 0.001 | | | |
| 5 ¹ A" | 3.660 | 339 | 0.031 | | | |
| 6 ¹ A′ | 3.714 | 334 | 0.001 | | | |
| 6 ¹ A" | 3.912 | 317 | 0.014 | | | |

involve a barrier at \sim 2.25 Å that arises from an avoided crossing with electronic excited states. On the 1 3 A″ state surface, the barrier to ground-state association to form the 1 3 A″ state of OAlNO is on the order of 0.5 eV (4000 cm $^{-1}$), requiring infrared activation of overtone and combination band transitions coupled with thermal activation. Alternatively, the singlet pathway needs to overcome a slightly higher barrier of \sim 0.75 eV (6050 cm $^{-1}$), suggesting that the triplet association pathway is the more kinetically and also thermodynamically favored pathway in addition to requiring less onerous infrared activation. The 1 3 A′ and 2 3 A″ states are repulsive and nearly degenerate in the Franck—Condon region, with predicted vertical excitation energies of 2.714 eV (457 nm) and 2.718 eV (456 nm), respectively.

The 1 ³A' state adiabatically correlates with the lowest dissociation limit products, while the 2 ³A" state adiabatically correlates with the first excited dissociation limit products AlO $(A^2\Pi)$ + NO $(X^2\Pi)$ and diabatically correlates with the more stable products. Electronic transition to both states has a predicted oscillator strength of 0.003, indicating weak but nonnegligible transition probability. Population of the 1 ³A' state would lead to direct dissociation to form AlO (X $^2\Sigma^+$) + NO $(X^2\Pi)$ products with the possibility of intersystem crossing to the 2 ¹A' state after which OAlNO would stabilize in a deep potential well since the 2 ¹A' state adiabatically correlates with the first excited-state product asymptote through a large barrier created by an avoided crossing with a higher-lying state. Excitation to the 2 ³A" state leads to immediate Al-N bond elongation and possible internal conversion to the 1 ³A" state and formation of ground-state AlO (X $^2\Sigma^+$) + NO (X $^2\Pi$)

products. Alternatively, if internal conversion does not occur, enough energy is supplied on the 2 $^3A'' \leftarrow 1$ $^3A''$ transition for dissociation to the excited-state products AlO (A $^2\Pi)$ + NO (X $^2\Pi)$ via overcoming the barrier at $\sim\!\!2.5$ Å created by interaction with the 4 $^3A''$ state. The 4 $^3A'' \leftarrow 1$ $^3A''$ transition is predicted to have the largest oscillator strength of 0.038, an order of magnitude larger than the transitions to the 2 $^3A''$ and 1 $^3A'$ states. However, excitation to the 4 $^3A''$ state leads to stabilization along the Al–N bond length due to the presence of a large dissociation barrier created by an avoided crossing with a higher state.

If formation of the 1 ¹A' state occurs, vertical excitation to the 4 ¹A' state is predicted to have a large oscillator strength of 0.031. The 4 ¹A' adiabatically correlates with a high-lying dissociation asymptote and will be stable. The 2 ¹A" and 3 ¹A' states both adiabatically correlate to the first excited-state asymptote and interact with the 1 1A" and 1 1A' states, respectively, via avoided crossings at ~2.25 Å. Electronic transitions to the 2 ¹A" and 3 ¹A' states are predicted to be very weak, with oscillator strengths of 0.001 and 0.002. However, population of these states leads to production of ground-state AlO (X $^2\Sigma^+$) + NO (X $^2\Pi$) products via nonadiabatic pathways or first excited-state products AlO (A $^{2}\Pi$) + NO (X $^{2}\Pi$) via adiabatic dissociation. Absorption of visible light in the 400-500 nm range, light readily available in the MLT region of the atmosphere, promotes electronic excitation and production of ground or excited-state AlO + NO products. Additionally, population of the higher-lying states leads to stabilization and fluorescence back down to the ground electronic state.

Moving to Figure 3b,c that depicts the evolution of the triplet and singlet states along the Al-O and N-O bond coordinates, the 1 3A" ground state is deeply bound in both the Al-O and N-O coordinates with bond dissociation energies of 5.25 eV (125.1 kcal mol⁻¹) and 7.10 eV (163.7 kcal mol^{-1}). Reaction of AlON + O (^{3}P) or OAlN + O (^{3}P) is extremely exothermic and would create a strong bonding interaction. The AlON and OAlN triatomic species may exist in the atmosphere through reactions such as AlO + N or Al + NO, 90 although further exploration is needed to validate these mechanisms. Thermal dissociation of the oxygen bonds is not possible due to the extreme dissociation energy. This behavior is in agreement with the preceding NBO analysis showing an NO triple bond and a strong AlO sigma bonding orbital. In Figure 3b, there is a cluster of triplet and singlet states within the 3-4 eV range of the Franck-Condon region that are all stable relative to the lowest energy dissociation asymptote. Above that, there are a few states that are stable relative to the next highest asymptote. All states have a deep well in the potential surface, and no Al-O bond fission will occur upon excitation to the excited states. Fluorescence with a minor Stokes shift from the upper states is the most favorable pathway, but phosphorescence is possible if intersystem crossing occurs in the crowded Franck-Condon region. The surfaces along the N-O bond length, shown in Figure 3c, depict similar behavior. The N-O bond is stronger than the Al-O bond in this case, causing the NAIO + O asymptote to be higher in energy. This makes all of the currently calculated excited states stable relative to the lowest dissociation asymptote, leading to stabilization along the N-O bond length.

Overall, the reaction of ground-state AlO and NO through the tetratomic OAlNO intermediate may lead to the photochemical production of electronically excited AlO in the MLT layer via the following pathway:

$$AIO(X^2\Sigma^+) + NO(X^2\Pi) \rightarrow OAINO + h\nu \rightarrow AIO(A^2\Pi) + NO(X^2\Pi)$$

This pathway will add to the concentration of electronically excited AlO, which is also produced via visible pumping on the B-X transition. In the MLT region of the atmosphere, with ubiquitous UV-vis light, the balance of weak absorption to the repulsive states leading to dissociation with strong absorption to fluorescing states and ground-state formation processes leads to questions of the steady-state concentration of OAINO in the atmosphere. There are many repulsive triplet and singlet states along the Al-N bond coordinate that will lead to the production of different electronic states for the AlO + NO products following electronic excitation of OAlNO in the visible (400-500 nm) region of the electromagnetic spectrum. These processes can occur through direct dissociation or nonadiabatic pathways. The stability of the higher-lying states suggests that excitation of the strong $4^{3}A'' \leftarrow 1^{3}A''$ transition will lead to fluorescence with a minor Stokes shift that can be utilized as a means of detection in an experimental setting. On the contrary, the excited-state topology along the Al-O and N-O bond coordinates predicts very stable bonds in all excited states and no Al-O or N-O bond dissociation following electronic excitation.

4. CONCLUSIONS

Production of OAINO may occur in the mesosphere and lower thermosphere of the earth's atmosphere via the reaction AlO + NO. AlO is produced by oxidation of Al atoms delivered via ablation of meteors and cosmic dust as they enter the atmosphere, while NO production occurs by the reaction of electronically excited N (2D) with O2 and exists at similar altitudes to AlO. OAlNO has a 3A" ground state leading to new and exciting spectroscopic and chemical implications for the earth's atmosphere. NBO analysis shows that the 1 ³A" state has an NO triple bond and two unpaired electrons in orthogonal oxygen p-orbitals that will make it reactive toward other species in the atmosphere. The 1 ¹A' state, which is an electronically excited state of OAlNO, has an AlO triple bond and NO double bond, an orbital configuration that causes slight destabilization and lower reactivity. Future studies that investigate the bimolecular chemistry of the 1 ³A" ground state with atmospheric species will further validate the impact that this novel aluminum species will have on the local MLT environment, potentially impacting climate science and highaltitude chemistry. For instance, this work implies that OAINO likely reduces nitrogen monoxide levels from the MLT, impacting NO_x chemistry in lower levels.

The 1 ³A" and 1 ¹A' states of OAlNO exhibit similar *B* rotational constants that may contribute to confusion for rotational spectra, thus requiring IR spectroscopic data as a differentiating tool. 1 ³A" and 1 ¹A' OAlNO and 1 ³A" OAlON contain notably intense vibrational transitions, with the largest being 1 ¹A' OAlNO's N-O stretch at 628 km mol⁻¹. 1 ¹A' OAlNO and 1 ³A" OAlON contain the most intense transitions of the three lowest energy species investigated. 1 ³A" and 1 ¹A' OAlNO and 1 ³A" OAlON exhibit very large dipole moments, the largest of which is 1 ³A" OAlNO at 3.82 D. However, with the confusion of the rotational spectra, the only species that may be characterized by its dipole moment would be the 1 ³A" OAlON as it still exhibits a large dipole of 2.66 D.

Exploration of the electronic excited states of OAlNO along the Al–O, Al–N, and N–O bond coordinates shows that excitation at prime solar wavelengths (400–500 nm) can lead to dissociation along the Al–N bond to form AlO + NO products via direct and nonadiabatic pathways, potentially impacting the chemistry of the earth's upper atmosphere. The formation of OAlNO via ground-state NO + AlO will lead to the photoproduction of electronically excited AlO in the mesosphere/lower thermosphere. The Al–O and N–O bonds are photostable, and excitation to the higher-lying states will lead to fluorescence with a minor Stokes shift that could be useful for future experimental detection in the laboratory.

ASSOCIATED CONTENT

Solution Supporting Information

The Supporting Information is available free of charge at https://pubs.acs.org/doi/10.1021/acs.jpca.3c04437.

Additional spectroscopic and thermodynamic information as well as Cartesian coordinates for all structures (PDF)

AUTHOR INFORMATION

Corresponding Author

Joseph S. Francisco — Department of Chemistry, University of Pennsylvania, Philadelphia, Pennsylvania 19104-6243, United States; orcid.org/0000-0002-5461-1486; Email: frjoseph@sas.upenn.edu

Authors

Vincent J. Esposito — Department of Chemistry, University of Pennsylvania, Philadelphia, Pennsylvania 19104-6243, United States; Present Address: NASA Ames Research Center, MS 245-3 Moffett Field, California 94035-1000, United States; © orcid.org/0000-0001-6035-3869

C. Zachary Palmer – Department of Chemistry and Biochemistry, University of Mississippi, University Park, Mississippi 38677-1848, United States

Ryan C. Fortenberry – Department of Chemistry and Biochemistry, University of Mississippi, University Park, Mississippi 38677-1848, United States; orcid.org/0000-0003-4716-8225

Complete contact information is available at: https://pubs.acs.org/10.1021/acs.jpca.3c04437

Notes

The authors declare no competing financial interest.

ACKNOWLEDGMENTS

This material is based upon work supported by the National Science Foundation Graduate Research Fellowship Program under Grant No. DGE-1845298 (V.J.E.). V.J.E.'s research was also supported by an appointment to the NASA Postdoctoral Program at NASA Ames Research Center, administered by the Oak Ridge Associated Universities through a contract with NASA. CZP and RCF acknowledge funding and support from NASA Grant NNX17AH15G, NSF Grant OIA-1757220, and the Mississippi Center for Supercomputing Research.

REFERENCES

(1) Mulliken, R. S. Electronic Structures of Polyatomic Molecules and Valence. II. Quantum Theory of the Double Bond. *Phys. Rev.* **1932**, *41*, 751–758.

- (2) Walsh, A. D. The Electronic Orbitals, Shapes, and Spectra of Polyatomic Molecules. Part 11. Non-Hydride AB, and BAC Molecdes. *J. Chem. Soc.* **1953**, 2266–2288.
- (3) Herzberg, G. The Bakerian Lecture, The Spectra and Structures of Free Methyl and Free Methylene. *Proc. R. Soc. London, Ser. A* **1961**, 291–317.
- (4) Bender, C. F.; Schaefer, H. F. New Theoretical Evidence for the Nonlinearity of the Triplet Ground State of Methylene. *J. Am. Chem. Soc.* 1970, 92, 4984–4985.
- (5) Wasserman, E.; Kuck, V. J.; Hutton, R. S.; Yager, W. A. Electron Paramagnetic Resonance of CD₂ and CHD. Isotope Effects, Motion, and Geometry of Methylene. *J. Am. Chem. Soc.* **1970**, *92*, 7491–7493.
- (6) Wasserman, E.; Yager, W. A.; Kuck, V. J. EPR of CH₂: A Substantially Bent and Partially Rotating Ground State Triplet. *Chem. Phys. Lett.* **1970**, *7*, 409–413.
- (7) Harrison, J. F.; Allen, L. C. Electronic Structure of Methylene. J. Am. Chem. Soc. 1969, 91, 807–823.
- (8) Bernheim, R. A.; Bernard, H. W.; Wang, P. S.; Wood, L. S.; Skell, P. S. Electron Paramagnetic Resonance of Triplet CH₂. *J. Chem. Phys.* **1970**, *53*, 1280–1281.
- (9) Herzberg, G.; Johns, J. W. C. On the Structure of CH₂ in Its Triplet Ground State. *J. Chem. Phys.* **1971**, *54*, 2276–2278.
- (10) Harrison, J. F. Structure of Methylene. Acc. Chem. Res. 1974, 7, 378–384.
- (11) Schaefer, H. F. Methylene: A Paradigm for Computational Quantum Chemistry. *Science* **1986**, 231, 1100–1107.
- (12) Wasserman, E. Mehylene: Experiment and Theory. Science 1986, 232, 1319.
- (13) Dowd, P.; Chang, W.; Paik, Y. H. Tetramethyleneethane, a Ground-State Triplet. J. Am. Chem. Soc. 1986, 108, 7416-7417.
- (14) Holthausen, M. C.; Koch, W.; Apeloig, Y. Theory Predicts Triplet Ground-State Organic Silylenes. *J. Am. Chem. Soc.* **1999**, *121*, 2623–2624.
- (15) Sun, J.; Abbenseth, J.; Verplancke, H.; Diefenbach, M.; de Bruin, B.; Hunger, D.; Würtele, C.; van Slageren, J.; Holthausen, M. C.; Schneider, S. A Platinum(II) Metallonitrene with a Triplet Ground State. *Nat. Chem.* **2020**, *12*, 1054–1059.
- (16) Esposito, V. J.; Trabelsi, T.; Francisco, J. S. Spectroscopic Properties Relevant to Astronomical and Laboratory Detection of MCH and MCH⁺ (M = Al, Mg). *Astrophys. J.* **2022**, *924*, 139.
- (17) Trabelsi, T.; Mahjoubi, K.; Mehnen, B.; Hochlaf, M.; Francisco, J. S. Spectroscopy and Stability of AlOP: A Possible Progenitor of Interstellar Metal. *J. Phys. Chem. A* **2019**, 123, 463–470.
- (18) Trabelsi, T.; Mahjoubi, K.; Mehnen, B.; Hochlaf, M.; Francisco, J. S. Spectroscopy and Characterization of AlNX (X = O and S): Triatomic Circumstellar Molecules. *J. Chem. Phys.* **2019**, *150*, No. 124306.
- (19) Kutzelnigg, W. Chemical Bonding in Higher Main Group Elements. *Angew. Chem., Int. Ed.* **1984**, 23, 272–295.
- (20) Doerksen, E. S.; Fortenberry, R. C. Coincidence between Bond Strength, Atomic Abundance, and the Composition of Rocky Materials. *ACS Earth Space Chem.* **2020**, *4*, 812–817.
- (21) Doerksen, E. S.; Fortenberry, R. C. Further Astrochemical Insights From Bond Strengths of Small Molecules Containing Atoms From the First Three Rows of the Periodic Table. *Front. Astron. Space Sci.* **2021**, *8*, No. 723530.
- (22) Plane, J. M. C.; Feng, W.; Dawkins, E. C. M. The Mesosphere and Metals: Chemistry and Changes. *Chem. Rev.* **2015**, *115*, 4497–4541.
- (23) Carrillo-Sánchez, J. D.; Gómez-Martín, J. C.; Bones, D. L.; Nesvorný, D.; Pokorný, P.; Benna, M.; Flynn, G. J.; Plane, J. M. C. Cosmic Dust Fluxes in the Atmospheres of Earth, Mars, and Venus. *Icarus* **2020**, 335, No. 113395.
- (24) Plane, J. M. C.; Daly, S. M.; Feng, W.; Gerding, M.; Gómez Martín, J. C. Meteor-Ablated Aluminum in the Mesosphere-Lower Thermosphere. J. Geophys. Res.: Space Phys. 2021, 126, No. e2020[A028792.
- (25) Mangan, T. P.; Harman-Thomas, J. M.; Lade, R. E.; Douglas, K. M.; Plane, J. M. C. Kinetic Study of the Reactions of AlO and OAlO

- Relevant to Planetary Mesospheres. ACS Earth Space Chem. 2020, 4, 2007–2017.
- (26) Esposito, V. J.; Francisco, J. S. The Photoionization Dynamics, Electronic Spectroscopy, and Excited State Photochemistry of AlCO and AlOC. *Astrophys. J.* **2022**, 933, 192.
- (27) Kiviranta, J.; Pérot, K.; Eriksson, P.; Murtagh, D. An Empirical Model of Nitric Oxide in the Upper Mesosphere and Lower Thermosphere Based on 12 Years of Odin SMR Measurements. *Atmos. Chem. Phys.* **2018**, *18*, 13393–13410.
- (28) Marsh, D. R.; Solomon, S. C.; Reynolds, A. E. Empirical Model of Nitric Oxide in the Lower Thermosphere. *J. Geophys. Res.: Space Phys.* **2004**, *109*, No. A07301.
- (29) Becke, A. D. Density-functional Thermochemistry. I. The Effect of the Exchange-only Gradient Correction. *J. Chem. Phys.* **1992**, *96*, 2155–2160.
- (30) Knowles, P. J.; Hampel, C.; Werner, H.-J. Coupled Cluster Theory for High Spin Open Shell Reference Wavefunctions. *J. Chem. Phys.* **1993**, *99*, 5219–5227.
- (31) Knowles, P. J.; Hampel, C.; Werner, H.-J. Erratum: "Coupled Cluster Theory for High Spin, Open Shell Reference Wave Functions" [J. Chem. Phys. **99**, 5219 (1993)]. *J. Chem. Phys.* **2000**, *112*, 3106–3107.
- (32) Dunning, T. H. Gaussian Basis Sets for Use in Correlated Molecular Calculations. I. The Atoms Boron through Neon and Hydrogen. *J. Chem. Phys.* **1989**, *90*, 1007–1023.
- (33) Dunning, T. H.; Peterson, K. A.; Wilson, A. K. Gaussian Basis Sets for Use in Correlated Molecular Calculations. X. The Atoms Aluminum through Argon Revisited. *J. Chem. Phys.* **2001**, *114*, 9244–9253.
- (34) Adler, T. B.; Knizia, G.; Werner, H.-J. A Simple and Efficient CCSD(T)-F12 Approximation. *J. Chem. Phys.* **2007**, *127*, No. 221106.
- (35) Knizia, G.; Adler, T. B.; Werner, H.-J. Simplified CCSD(T)-F12 Methods: Theory and Benchmarks. *J. Chem. Phys.* **2009**, *130*, No. 054104.
- (36) Peterson, K. A.; Adler, T. B.; Werner, H.-J. Systematically Convergent Basis Sets for Explicitly Correlated Wavefunctions: The Atoms H, He, B-Ne, and Al-Ar. *J. Chem. Phys.* **2008**, *128*, No. 084102.
- (37) Werner, H.-J.; Knowles, P. J.; Knizia, G.; Manby, F. R.; Schütz, M.; Celani, P.; Györffy, W.; Kats, D.; Korona, T.; Lindh, R.et al. *MOLPRO, Version 2021, A Package of Ab Initio Programs*; MOLPRO, 2021.
- (38) Glendening, E. D.; Badenhoop, J. K.; Reed, A. E.; Carpenter, J. E.; Bohmann, J. A.; Morales, C. M.; Karafiloglou, P.; Landis, C. R.; Weinhold, F. *NBO 7.0*; Theoretical Chemistry Institute, University of Wisconsin, Madison; 2018.
- (39) Grimme, S.; Ehrlich, S.; Goerigk, L. Effect of the Damping Function in Dispersion Corrected Density Functional Theory. *J. Comput. Chem.* **2011**, 32, 1456–1465.
- (40) Goerigk, L.; Grimme, S. Efficient and Accurate Double-Hybrid-Meta-GGA Density Functionals—Evaluation with the Extended GMTKN30 Database for General Main Group Thermochemistry, Kinetics, and Noncovalent Interactions. *J. Chem. Theory Comput.* **2011**, *7*, 291–309.
- (41) Frisch, M. J.; Trucks, G. W.; Schlegel, H. B.; Scuseria, G. E.; Robb, M. A.; Cheeseman, J. R.; Scalmani, G.; Barone, V.; Petersson, G. A.; Nakatsuji, H.et al. *Gaussian 16*; Gaussian, Inc.: Wallingford, CT, 2016.
- (42) Fortenberry, R. C.; Lee, T. J. Computational Vibrational Spectroscopy for the Detection of Molecules in Space. In *Annual Reports in Computational Chemistry*; Dixon, D. A., Ed.; Elsevier, 2019; Vol. 15, pp 173–202.
- (43) Huang, X.; Lee, T. J. A Procedure for Computing Accurate Ab Initio Quartic Force Fields: Application to HO_2^+ and H_2O . *J. Chem. Phys.* **2008**, *129*, No. 044312.
- (44) Huang, X.; Lee, T. J. Accurate Ab Initio Quartic Force Fields for NH₂⁻ and CCH⁻ and Rovibrational Spectroscopic Constants for Their Isotopologs. *J. Chem. Phys.* **2009**, *131*, No. 104301.

- (45) Huang, X.; Taylor, P. R.; Lee, T. J. Highly Accurate Quartic Force Fields, Vibrational Frequencies, and Spectroscopic Constants for Cyclic and Linear C₃H₃⁺. *J. Phys. Chem. A* **2011**, *115*, 5005–5016.
- (46) Zhao, D.; Doney, K. D.; Linnartz, H. Laboratory Gas-Phase Detection of the Cyclopreopenyl Cation. *Astrophys. J.* **2014**, 791, No. L28.
- (47) Huang, X.; Fortenberry, R. C.; Lee, T. J. Protonated Nitrous Oxide, NNOH⁺: Fundamental Vibrational Frequencies and Spectroscopic Constants from Quartic Force Fields. *J. Chem. Phys.* **2013**, *139*, No. 084313.
- (48) Fortenberry, R. C.; Huang, X.; Crawford, T. D.; Lee, T. J. Quartic Force Field Rovibrational Analysis of Protonated Acetylene, $C_2H_3^+$, and Its Isotopologues. *J. Phys. Chem. A* **2014**, *118*, 7034–7043.
- (49) Fortenberry, R. C.; Lee, T. J.; Müller, H. S. P. Excited Vibrational Level Rotational Constants for SiC_2 : A Sensitive Molecular Diagnostic for Astrophysical Conditions. *Mol. Astrophys.* **2015**, *1*, 13–19.
- (50) Kitchens, M. J. R.; Fortenberry, R. C. The Rovibrational Nature of Closed-Shell Third-Row Triatomics: HOX and HXO, $X = Si^+$, P, S^+ , and Cl. Chem. Phys. **2016**, 472, 119.
- (51) Fortenberry, R. C. Quantum Astrochemical Spectroscopy. *Int. J. Quantum Chem.* **2017**, *117*, 81–91.
- (52) Fortenberry, R. C.; Novak, C. M.; Layfield, J. P.; Matito, E.; Lee, T. J. Overcoming the Failure of Correlation for Out-of-Plane Motions in a Simple Aromatic: Rovibrational Quantum Chemical Analysis of c-C₃H₃. J. Chem. Theory Comput. **2018**, 14, 2155–2164.
- (53) Gardner, M. B.; Westbrook, B. R.; Fortenberry, R. C.; Lee, T. J. Highly-Accurate Quartic Force Fields for the Prediction of Anharmonic Rotational Constants and Fundamental Vibrational Frequencies. *Spectrochim. Acta, Part A* **2021**, 248, No. 119184.
- (54) Raghavachari, K.; Trucks, G. W.; Pople, J. A.; Head-Gordon, M. A Fifth-Order Perturbation Comparison of Electron Correlation Theories. *Chem. Phys. Lett.* **1989**, *157*, 479–483.
- (55) Martin, J. M. L.; Kesharwani, M. K. Assessment of CCSD(T)-F12 Approximations and Basis Sets for Harmonic Vibrational Frequencies. *J. Chem. Theory Comput.* **2014**, *10*, 2085–2090.
- (56) Agbaglo, D.; Lee, T. J.; Thackston, R.; Fortenberry, R. C. A Small Molecule with PAH Vibrational Properties and a Detectable Rotational Spectrum: *C*-(C)C₃H₂, Cyclopropenylidenyl Carbene. *Astrophys. J.* **2019**, *871*, 236.
- (57) Agbaglo, D.; Fortenberry, R. C. The Performance of Explicitly Correlated Methods for the Computation of Anharmonic Vibrational Frequencies. *Int. J. Quantum Chem.* **2019**, *119*, No. e25899.
- (58) Palmer, C. Z.; Fortenberry, R. C.; Francisco, J. S. Spectral Signatures of Hydrogen Thioperoxide (HOSH) and Hydrogen Persulfide (HSSH): Possible Molecular Sulfur Sinks in the Dense ISM. *Molecules* **2022**, *27*, No. 3200.
- (59) Westbrook, B. R.; Dreux, K. M.; Tschumper, G. S.; Francisco, J. S.; Fortenberry, R. C. Binding of the Atomic Cations Hydrogen through Argon to Water and Hydrogen Sulfide. *Phys. Chem. Chem. Phys.* **2018**, 20, 25967–25973.
- (60) Inostroza-Pino, N.; Palmer, C. Z.; Lee, T. J.; Fortenberry, R. C. Theoretical Rovibrational Characterization of the Cis/Trans-HCSH and H₂SC Isomers of the Known Interstellar Molecule Thioformal-dehyde. *J. Mol. Spectrosc.* **2020**, *369*, No. 111273.
- (61) Agbaglo, D.; Fortenberry, R. C. The Performance of Explicitly Correlated Wavefunctions [CCSD(T)-F12b] in the Computation of Anharmonic Vibrational Frequencies. *Chem. Phys. Lett.* **2019**, 734, No. 136720.
- (62) Hill, J. G.; Peterson, K. A. Correlation Consistent Basis Sets for Explicitly Correlated Wavefunctions: Valence and Core–Valence Basis Sets for Li, Be, Na, and Mg. *Phys. Chem. Chem. Phys.* **2010**, *12*, 10460
- (63) Watrous, A. G.; Westbrook, B. R.; Fortenberry, R. C. F12-TZ-CCR: A Methodology for Faster and Still Highly Accurate Quartic Force Fields. *J. Phys. Chem. A* **2021**, *125*, 10532–10540.

- (64) Westbrook, B. R.; Fortenberry, R. C. Anharmonic Vibrational Frequencies of Water Borane and Associated Molecules. *Molecules* **2021**, *26*, No. 7348.
- (65) Palmer, C. Z.; Fortenberry, R. C. Fluoro Hydrogen Peroxide: A Plausible Molecular Form of Naturally-Occurring Fluorine. *ACS Earth Space Chem.* **2022**, *6*, 2032.
- (66) Werner, H.-J.; Knowles, P. J.; Knizia, G.; Manby, F. R.; Schütz, M.; Celani, P.; Györffy, W.; Kats, D.; Korona, T.; Lindh, R.et al. *MOLPRO, Version 2020.1, A Package of Ab Initio Programs*; MOLPRO, 2020.
- (67) Allen, W. D., et al. INTDER, 2005.
- (68) Fortenberry, R. C.; Trabelsi, T.; Francisco, J. S. Anharmonic Frequencies and Spectroscopic Constants of OAlOH and AlOH: Strong Bonding but Unhindered Motion. *J. Phys. Chem. A* **2020**, *124*, 8834–8841.
- (69) Douglas, M.; Kroll, N. M. Quantum Electrodynamic Corrections to the Fine Structure of Helium. *Ann. Phys.* **1974**, *82*, 89–155.
- (70) Gaw, J. F.; Willetts, A.; Green, W. H.; Handy, N. C. SPECTRO a Program for Derivation of Spectroscopic Constants from Provided Quartic Force Fields and Cubic Dipole Fields. *Advances in Molecular Vibrations and Collision Dynamics*; JAI Press, 1991; pp 169–185.
- (71) Mills, I. In Molecular Spectroscopy: Modern Research; Rao, N.; Mathews, C. W., Eds.; Academic Press, 1972.
- (72) Papousek, D.; Aliey, M. R. Molecular Vibration-Rotation Spectra; Elsevier: Amsterdam, 1982.
- (73) Watson, J. K. G. On Vibrational Spectra and Structure; Elsevier: Amsterdam, 1977.
- (74) Hehre, W. J.; Ditchfield, R.; Pople, J. A. Self—Consistent Molecular Orbital Methods. XII. Further Extensions of Gaussian—Type Basis Sets for Use in Molecular Orbital Studies of Organic Molecules. *J. Chem. Phys.* **1972**, *56*, 2257–2261.
- (75) Yu, Q.; Bowman, J. M.; Fortenberry, R. C.; Mancini, J. S.; Lee, T. J.; Crawford, T. D.; Klemperer, W.; Francisco, J. S. Structure, Anharmonic Vibrational Frequencies, and Intensities of NNHNN⁺. *J. Phys. Chem. A* **2015**, *119*, 11623–11631.
- (76) Finney, B.; Fortenberry, R. C.; Francisco, J. S.; Peterson, K. A. A Spectroscopic Case for SPSi Detection: The Third-Row in a Single Molecule. *J. Chem. Phys.* **2016**, *145*, No. 124311.
- (77) Westbrook, B. R.; Patel, D. J.; Dallas, J. D.; Swartzfager, G. C.; Lee, T. J.; Fortenberry, R. C. Fundamental Vibrational Frequencies and Spectroscopic Constants of Substituted Cyclopropenylidene (c-C₃HX, X = F, Cl, CN). *J. Phys. Chem. A* **2021**, 125, 8860–8868.
- (78) Knowles, P. J.; Werner, H.-J. An Efficient Method for the Evaluation of Coupling Coefficients in Configuration Interaction Calculations. *Chem. Phys. Lett.* **1988**, *145*, 514–522.
- (79) Shamasundar, K. R.; Knizia, G.; Werner, H.-J. A New Internally Contracted Multi-Reference Configuration Interaction Method. *J. Chem. Phys.* **2011**, *135*, No. 054101.
- (80) Werner, H.-J.; Knowles, P. J. An Efficient Internally Contracted Multiconfiguration Reference CI Method. *J. Chem. Phys.* **1988**, *89*, 5803–5814.
- (81) Szalay, P. G.; Bartlett, R. J. Multi-Reference Averaged Quadratic Coupled-Cluster Method: A Size-Extensive Modification of Multi-Reference CI. *Chem. Phys. Lett.* **1993**, *214*, 481–488.
- (82) Knowles, P. J.; Werner, H.-J. An Efficient Second Order MCSCF Method for Long Configuration Expansions. *Chem. Phys. Lett.* **1985**, *115*, 259–267.
- (83) Werner, H.-J.; Knowles, P. J. A Second Order MCSCF Method with Optimum Convergence. *J. Chem. Phys.* **1985**, 82, 5053.
- (84) Li, S.; Sattelmeyer, K. W.; Yamaguchi, Y.; Schaefer, H. F. Characterization of the Three Lowest-Lying Singlet Electronic States of AlOH. *J. Chem. Phys.* **2003**, *119*, 12830–12841.
- (85) Apponi, A. J.; Barclay, W. L., Jr.; Ziurys, L. M. The Milimeter Wave Spectrum of AlOH. *Astrophys. J. Lett.* **1993**, 414, L129–L132.
- (86) Wang, X.; Andrews, L. Infrared Spectroscopic Observation of the Group 13 Metal Hydroxides, M(OH)_{1,2,3} (M = Al, Ga, In, and Tl) and HAl(OH)₂. *J. Phys. Chem. A* **2007**, *111*, 1860–1868.

- (87) Hollman, D. S.; Schaefer, H. F. In Search of the next Holy Grail of Polyoxide Chemistry: Explicitly Correlated *Ab Initio* Full Quartic Force Fields for HOOH, HOOOH, HOOOOH, and Their Isotopologues. *J. Chem. Phys.* **2012**, *136*, No. 084302.
- (88) Fortenberry, R. C.; Huang, X.; Francisco, J. S.; Crawford, T. D.; Lee, T. J. Fundamental Vibrational Frequencies and Spectroscopic Constants of HOCS⁺, HSCO⁺, and Isotopologues via Quartic Force Fields. *J. Phys. Chem. A* **2012**, *116*, 9582–9590.
- (89) Fortenberry, R. C.; Huang, X.; Francisco, J. S.; Crawford, T. D.; Lee, T. J. Quartic Force Field Predictions of the Fundamental Vibrational Frequencies and Spectroscopic Constants of the Cations HOCO⁺ and DOCO⁺. *J. Chem. Phys.* **2012**, *136*, No. 234309.
- (90) Zhang, L.; Zhou, M. Theoretical Investigation on the Potential Energy Surface for the Reactions of B, Al and Ga with NO. *Chem. Phys.* **2000**, 256, 185–194.
- (91) Gómez Martín, J. C.; Daly, S. M.; Brooke, J. S. A.; Plane, J. M. C. Absorption Cross Sections and Kinetics of Formation of AlO at 298 K. Chem. Phys. Lett. 2017, 675, 56–62.

☐ Recommended by ACS

Reaction of Atmospherically Relevant Sulfur-Centered Radicals with RO_2 and HO_2

Jing Chen, Henrik G. Kjaergaard, et al.

MARCH 28, 2023

THE JOURNAL OF PHYSICAL CHEMISTRY A

READ 🗹

Secondary Organic Aerosol (SOA) through Uptake of Isoprene Hydroxy Hydroperoxides (ISOPOOH) and its Oxidation Products

Peter Mettke, Hartmut Herrmann, et al.

APRIL 25, 2023

ACS EARTH AND SPACE CHEMISTRY

READ 🗹

Growth Rate Dependence of Secondary Organic Aerosol on Seed Particle Size, Composition, and Phase

Devon N. Higgins, Murray V. Johnston, et al.

AUGUST 10, 2022

ACS EARTH AND SPACE CHEMISTRY

RFAD **[**✓

Theoretical Investigations of the OH-Initialized Oxidation of 4-Methyl-3-Penten-2-One in the Atmosphere

Benni Du and Weichao Zhang

AUGUST 26, 2022

ACS EARTH AND SPACE CHEMISTRY

READ 🗹

Get More Suggestions >